Taylor & Francis
Taylor & Francis Group

Investigation of apoptosis in cultured cells infected with equine herpesvirus 1

MR Scrochi[1,2,6], CN Zanuzzi[2,3,6], N Fuentealba[1,6], F Nishida[3], ME Bravi[1,6], ME Pacheco[5,6], GH Sguazza[1], EJ Gimeno[3,6], EL Portiansky[3,6], CI Muglia[4,6], CM Galosi[1,7], CG Barbeito[2,6]

[1]*Departments of Virology*, [2]*Histology and Embryology*, [3]*Image Analysis Laboratory, School of Veterinary Sciences, National University of La Plata, La Plata*, [4]*Department of Immunopathology, Institute of Immunological and Physiopathological Studies (IIFP)*, [5]*Department of Analytical Chemistry, School of Exact Sciences, National University of La Plata, La Plata*, [6]*National Scientific and Technical Research Council (CONICET), Argentina, and* [7]*Scientific Research Commission of Buenos Aires Province (CIC-PBA), Buenos Aires, Argentina*

Abstract

Many viruses alter different stages of apoptosis of infected cells as a strategy for successful infection. Few studies have addressed mechanisms of equine herpesvirus 1 (EHV-1) strain-induced cell death. We investigated the effect of an abortigenic strain (AR8 strain) on heterologous Madin–Darby bovine kidney cells and homologous equine dermis (ED) cells cell lines. We compared morphologic and biochemical features of early and late apoptosis at different postinfection times. We investigated translocation of phosphatidylserine to the cell surface, nuclear fragmentation and changes in the cytoskeleton using flow cytometry and annexin V/propidium iodide staining, DNA laddering, terminal deoxynucleotidyl transferase UTP nick-end labeling assay and immunofluorescence staining of cytokeratin 18 cleavage. AR8 EVH-1 strain interfered with apoptosis in both cell lines, particularly during the middle stage of the replication cycle; this was more evident in ED cells. Although this antiapoptotic effect has been reported for other alpha herpesviruses, our findings may help elucidate how EHV-1 improves its infectivity during its cycle.

Key words: apoptosis, equine dermis cells, equine herpes virus 1, Madin–Darby bovine kidney cells

Apoptosis frequently is initiated by viral infection (Miles et al. 2007). Many viruses alter different stages of apoptosis in infected cells as a strategy for successful infection (Aubert et al. 2007, De Martino et al. 2003, Munger et al. 2001, Perng et al. 2000). Alteration of apoptosis of infected host cells may prevent premature death of the virus, which enables it to replicate and establish a latent phase. Proapoptotic mechanisms may be activated, however, to enhance efficient diffusion of viral progeny to neighboring cells (Cheung et al. 2000, Longo et al. 2009, Pagnini et al. 2005). Owing to the importance of this process, many techniques have been developed to identify early and late stages of apoptosis.

Equine herpesvirus-1 (EHV-1) belongs to the genus, *Varicellovirus*, subfamily, *Alpha herpesvirinae*. Infection in horses is associated with clinical manifestations including rhinopneumonitis, abortion, neonatal death and neurological disease. As with other alpha herpesviruses, EHV-1 can cause latent infections in trigeminal ganglia that are reactivated under stressful situations (Allen et al. 2004). EHV-1 expresses genes known as immediate early, early and late genes. Their sequential expression is important for a successful viral replication cycle (Honess and Roizman 1974). Their possible implications for regulation of infected cell survival, however, remain unknown.

Correspondence: Claudio G. Barbeito, Histology and Embryology, School of Veterinary Sciences, National University of La Plata, 60 and 118 Postal code 1900, La Plata, Buenos Aires, Argentina. E-mail: barbeito@fcv.unlp.edu.ar

Biotechnic & Histochemistry 2017, **Early Online:** 1–9

It has been reported that different alpha herpesviruses, including herpes simplex virus 1 (HSV-1) (Aubert and Blaho 1999, Galvan et al. 1999, Miles et al. 2007), suid herpesvirus 1 (SuHV-1) (Deruelle et al. 2010) and bovine herpesvirus 1 (BoHV-1) (De Martino et al. 2003) regulate apoptosis in infected cells. Cymerys et al. (2012) reported that EHV-1 exhibited an inhibitory effect on apoptosis in neuronal cell cultures, which might be associated with establishment of the latency phase. Building upon our previous investigation using heterologous cell lines and Japanese EHV-1 HH1 strain (Scrochi et al. 2013), we evaluated the effect of EHV-1 on two cell lines during replication to characterize further its effect on host cell apoptosis.

Material and methods

Cell culture

We used Madin–Darby bovine kidney (MDBK) cells (ABAC, Argentine Cell Bank Association, Argentina) to study a heterologous cell line model and an homologous cell line model was developed using equine dermis (ED) cells provided by the Butantan Institute (Sao Paulo, Brazil). Both cell lines were grown in minimum essential medium (MEM) (Gibco, Invitrogen, Carlsbad, CA), supplemented with 2 mM glutamine (Gibco, Invitrogen), 100 IU/ml penicillin, 100 µg/ml streptomycin (Ritchet, Buenos Aires, Argentina), 100 IU/ml nystatin (Parafarm, Buenos Aires, Argentina) and 10% fetal calf serum (FCS). FCS was reduced to 2% (M-MEM) for cell maintenance. Cells were harvested with trypsin (0.25% w/v)-EDTA (0.2% w/v) (Sigma-Aldrich, St Louis, MO) and viability was assessed using trypan blue staining and optical microscopy.

Virus strain

The Argentinean AR8 strain used for all assays was obtained from our virus collection (Department of Virology, School of Veterinary Sciences, National University of La Plata). The virus was isolated in 1996 from one of several aborted equine fetuses on an Argentinean farm (data not published). The strain was maintained in RK13 rabbit kidney cells with M-MEM. A genomic study of several strain regions showed no changes compared to the Ab4 and V592 strains (Fuentealba et al. 2011).

Confluent monolayers of RK13 cells were grown in individual T25 flasks (Cellstar, Frickenhausen, Germany), infected with AR8 strain and incubated with M-MEM at 37° C in a 5% CO_2 atmosphere. When extensive cytopathic effect was observed, the flasks were frozen at −70° C. After three cycles of freezing and thawing, the cells and infectious supernatant were centrifuged at 8000 × *g* for 20 min to remove cell debris. The final infectious supernatant was fractionated in small volumes and stored at −70° C until use. Virus titer was determined using the Reed and Muench method (Reed and Muench 1938). Viral suspension was incubated for 1 h at 37° C with either cell line at a multiplicity of infection of 10 $CCID_{50}$ (Deruelle et al. 2010, Soboll Hussey et al. 2014). Subsequently, the inoculum was removed and cells were washed with FCS-free medium and re-incubated with M-MEM at 37° C in a 5% CO_2 atmosphere for 3, 9 or 18 h postinfection. In uninfected groups, the viral inoculum was replaced by M-MEM. Infected MDBK and ED cells were collected at 0, 3, 9 and 18 h postinfection for total DNA determination using a Wizard Genomic DNA Purification Kit (Promega, Madison, WI) according to manufacturer's protocol.

Infection of MDBK and ED cells by EHV-1

To verify viral replication, the number of glycoprotein C (gpC) gene copies was determined using quantitative real-time PCR (qPCR). qPCR was performed using a pair of specific oligonucleotide primers that amplified a 369-bp fragment derived from a conserved gpC region of EHV-1: 5′-CAAC AATCGGGGAGGCGTCATA-3′ (position 21582–21603) and 5′-GTAGCATAGACTGGTACAGGGA-3′ (position 21929–21950).

Amplification was accomplished using a previously standardized protocol (Galosi et al. 2001) that uses SYBR® Green (Applied Biosystems, Foster City, CA) and an iCycler (Bio-Rad, Sacramento, CA). The presence of viral particles also was evaluated by transmission electron microscopy (TEM). At 9 h postinfection, infected cells were scraped, fixed with buffered glutaraldehyde for 2 h at 4° C, then treated with osmium tetroxide. Samples were observed using a JEM 1200 EX II (Tokyo, Japan) electron microscope.

Experimental design

For each cell line, several experimental groups, grown on either coverslips or in flasks, were analyzed at specific times. Uninfected cells (Cc) were

used as controls. Cell lines in which apoptosis was induced (Apo+) were positive controls. For this purpose, cells were incubated with 1 M sorbitol for 1 h at 37° C (De Martino et al. 2003, 2007). Subsequently, sorbitol was removed, monolayers were washed twice with MEM for 5 min each and incubation was continued in M-MEM for 2 h at 37° C until further analysis. Experimentally infected cell (Inf) samples were taken at 3, 9 and 18 h incubation.

Morphological analysis of apoptosis

Flask-cultured cells, 5×10^5 cells/ml, were harvested with trypsin-EDTA for 5 min at 37° C at each time point postinfection. After washing twice in phosphate-buffered saline (PBS), 50 µl of the supernatant containing approximately 12,500 viable cells was mixed with 3 µl 200 µg/ml acridine orange + 200 µg/ml ethidium bromide (Sigma-Aldrich) solution. Then, 5 µl of each sample was spread on a slide and quantified under a wide field microscope (BX51, Olympus Co., Tokyo, Japan) using a PlanFluorite, NA 0.75, 40 × objective. Normal and early apoptotic cells were stained bright green by acridine orange, whereas late apoptotic cells were stained bright orange by ethidium bromide.

DNA fragmentation assay for apoptosis

Cells were harvested with trypsin-EDTA and DNA extraction was performed using the Wizard Genomic DNA Purification Kit (Promega), according to manufacturer's protocol. Electrophoresis of the sample was performed on 1.5% agarose gel for 4 h at 80 V, stained with 0.5 µg/ml ethidium bromide and visualized under UV light. Band size was calculated compared to a standard 100 bp molecular weight marker (Invitrogen, Milan, Italy). Fragments 100–200 bp indicated internucleosomal DNA fragmentation.

Annexin V/Propidium iodide staining analysis by flow cytometry

Early stages of apoptosis were quantified by flow cytometry using annexin V-FITC/propidium iodide double staining. Use of propidium iodide with annexin V distinguishes viable, apoptotic and necrotic cells by differences in plasma membrane integrity and permeability. Annexin V-FITC binds to phosphatidylserine and indicates early apoptosis, whereas propidium iodide staining indicates necrosis. Cells were removed with scrapers, washed twice with PBS, incubated for 20 min with annexin V-FITC (BD Biosciences, San Jose, CA) in the dark, then propidium iodide was added just before quantification. In this way, early (annexin V+/propidium iodide–) and late (annexin V +/propidium iodide+) apoptotic events were quantified. Fluorescence was detected using a FACS Calibur cytometer (BD Pharmigen, Becton, Dickinson Co., Franklin Lakes, NJ). A homogeneous cell population was gated using forward scatter/side scatter in control samples. Then, the same gate was used for all samples.

Terminal deoxynucleotidyl transferase UTP nick end labeling (TUNEL)

DNA is cleaved during apoptosis. TUNEL is used to detect fragmentation of nuclear chromatin at a late stage of apoptosis, which results in myriad 3′-hydroxyl termini of DNA. Cells grown on coverslips and fixed with acetone were incubated for 1 h at 37° C using the in situ cell death detection kit TMR red (Roche, Mannheim, Germany) according to the manufacturer's instructions. Cells then were washed twice with PBS containing 0.5% Tween 20 (Merck, Schuchardt OHG, Hohenbrunn, Germany). Nuclei were counterstained with 5 µg/ml 6-diamidino-2-phenylindole (DAPI) (Invitrogen Life Technologies, Eugene, OR). Coverslips were mounted on slides using the aqueous medium, Reagent FluoroSave™ (Calbiochem, La Jolla, CA), then examined using confocal microscopy (FV1000; Olympus Co.). Images were taken using a 40 ×, NA 0.95 UPLSAPO objective. Filters were used for emission of the fluorophore: Texas red (red) (laser 559 nm) and DAPI (blue) (laser 405 nm). For each experiment, 1000 cells were scored and labeled cells were quantified using an image analyzer (cellSens Dimension v1.6; Olympus Co.). Apoptotic cells were stained with the Texas red fluorophore. No further processing was used. Apoptotic and non-apoptotic cells were counted using the automatic histogram function of software.

Cleavage for cytokeratin 18

During early apoptosis, cytokeratin 18 is cleaved by caspases, which liberates a neo-epitope that is recognized specifically by M30 CytoDEATH monoclonal antibody (Roche). Assays were performed according to the manufacturer's instructions.

Briefly, cells grown on coverslips and fixed with acetone were incubated for 1 h at 37° C with the mouse monoclonal antibody, M30CytoDeath, diluted 1:10 with 0.1% bovine serum albumin (BSA). The cells were washed twice with PBS containing 0.5% Tween 20 (Merck) and incubated for 1 h at 37° C with Alexafluor™ 488 goat anti-mouse antibody (Invitrogen Life Technologies, Eugene, OR) diluted 1:1000 with 0.1% BSA. DAPI was used for nuclear staining. Coverslips were mounted on slides using the aqueous medium, Reagent FluoroSave™, then examined using confocal microscopy. The labeled cells were quantified using an image analyzer. Each experiment was repeated three times and results were recorded as means ± SD.

Statistical analysis

Results were expressed as means ± SD. Student's *t*-test and one-way ANOVA followed by the LSD *post hoc* test were used for data analysis. Values for $p \leq 0.05$ were considered significant.

Results

Infection of MDBK and ED Cells by EHV-1

A significant increase was observed in the number of gpC gene copies determined by qPCR from 3 to 18 h postinfection in both cells lines (Fig. 1). After 18 h postinfection, cells showed a cytopathic effect (Fig. 2). Viral particles were detected in both MDBK and ED cells using TEM (Fig. 3).

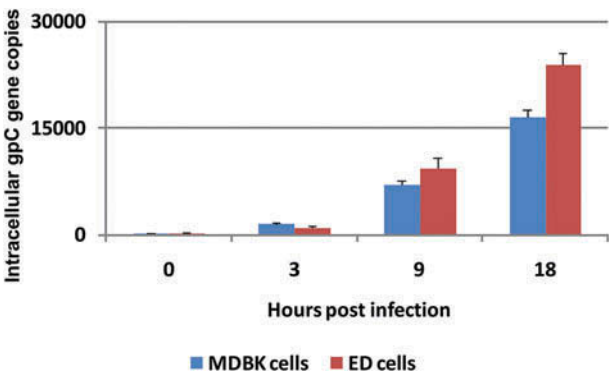

Fig. 1. gpC copy numbers obtained by qPCR from MDBK and ED cells infected with EHV-1 strain and analyzed at 0, 3, 9 or 18 h postinfection.

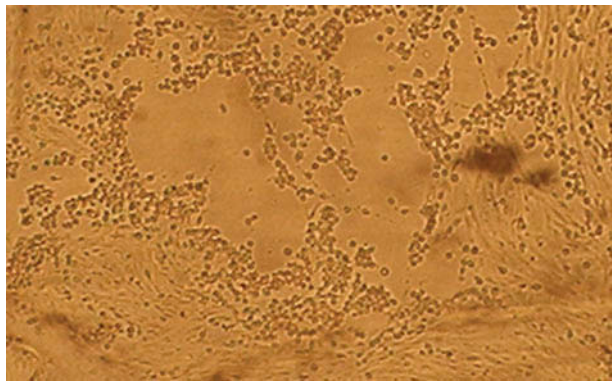

Fig. 2. Cytopathic effect in MDBK cells at 18 h postinfection with EHV-1.

Morphological analysis of apoptosis

For MDBK cells, the Inf groups showed a greater number of apoptotic cells than the corresponding Cc, but significant differences were observed only at 18 h postinfection ($p < 0.05$) (Fig. 4).

For ED cells, apoptosis was significantly greater in the Inf groups at 3 and 9 h postinfection than in the Cc groups.

DNA fragmentation assay of apoptosis

DNA fragmentation was observed in the Apo+ groups of MDBK and ED cells; however, in the Inf groups, DNA fragmentation was detected only at 18 h postinfection for both cell lines (Fig. 5).

Annexin V/PI staining and flow cytometry

For MDBK cells, no significant differences in the percentages of annexin V+/PI– cells were observed between the Cc and Inf groups at the time points examined. At 9 h postinfection, however, the Inf group exhibited a significantly lower percentage of annexin V+/PI– than the Apo+ group ($p < 0.01$).

For ED cells, the percentage of annexin V+/PI– cells was significantly lower at 3 and 9 h than at 18 h postinfection in the Inf groups ($p < 0.01$) (Fig. 6).

TUNEL assay

For MDBK cells, no significant difference in the number of TUNEL positive cells was found between the Inf and Cc groups at any time studied. At 9 h postinfection, however, we found a lower percentage of TUNEL positive cells compared to 3 and 18 h postinfection.

For ED cells, the percentage of TUNEL positive cells was significantly increased at 3 and 18 h

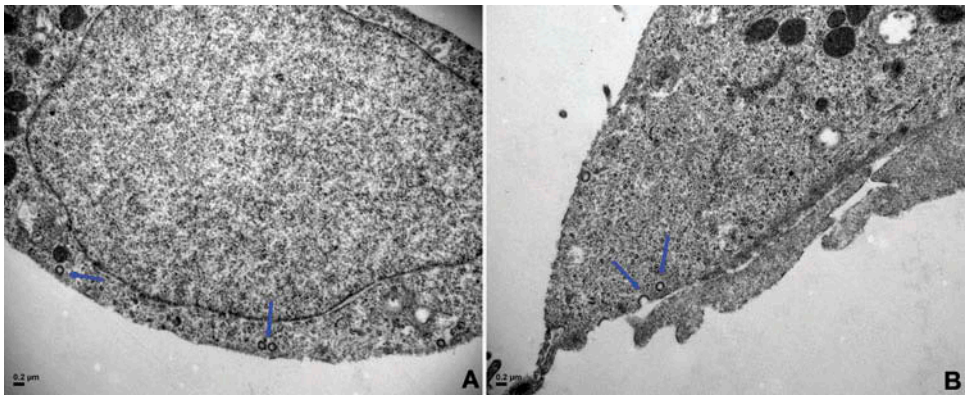

Fig. 3. Transmission electron micrographs infected MDBK (a) and ED cells (b) at 9 h postinfection. Arrows, viral particles.

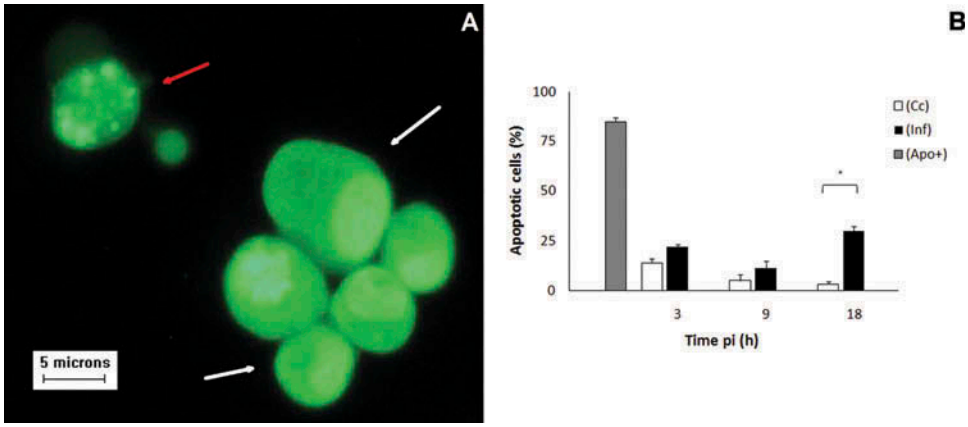

Fig. 4. Morphological analysis of EHV-1-infected MDBK cells stained with acridine orange and ethidium bromide. a) Early apoptotic cells are stained bright green by acridine orange at 18 h postinfection. White arrows show normal cell, whereas red arrow shows apoptotic cell. b) Apoptotic rate using acridine orange and ethidium bromide staining. Statistically significant differences (*) between 18 h Inf and the corresponding Cc group, $p < 0.01$.

compared to the Cc groups ($p < 0.001$). Among all infected groups, at 9 h post infection, we found a significantly lower percentage of TUNEL positive cells ($p < 0.001$) (Fig. 7).

Cleavage for cytokeratin 18

For MDBK cells, we found no significant differences in cytokeratin 18 staining between the Inf and Cc groups at any time postinfection, although at 9 h postinfection, a lower percentage of positive cells was found in the infected cells.

For ED cells, the percentage of positive M30 cells in the Cc and Inf groups was reduced significantly at 9 h but increased at 18 h ($p < 0.01$); the highest percentage was found at 18 h ($p < 0.01$) (Fig. 8).

Discussion

It has been reported that alpha herpesviruses interfere with the apoptotic process of infected cells to promote viral replication and survival (De Martino et al. 2003, Deruelle et al. 2010). Some investigators have analyzed changes in the cytoskeleton during the infection process. Deruelle et al. (2010) reported that SuHV-1 may be involved in multiple interactions with the actin cytoskeleton to increase replication efficiency in swine testis cells. Similar observations have been reported for EHV-1 strains in ED and Vero cell lines (Turowska et al. 2010) and in infected primary murine neurons (Słonska et al. 2014). On the other hand, the literature contains conflicting reports regarding the effects of EHV-1 on apoptosis of cultured cells. Also, little is known about how in vitro

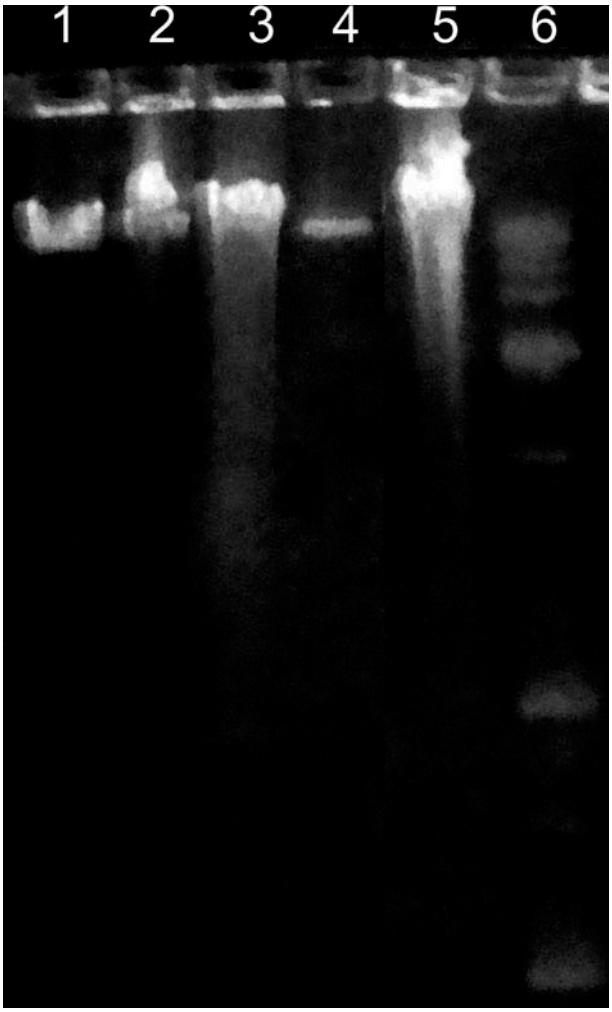

Fig. 5. DNA fragmentation in MDBK cells. (Inf) at 3 (1), 9 (2) and 18 h (3) postinfection, Cc (4), Apo+ (5) and molecular marker (6). DNA fragmentation was observed in the Inf group at 18 h postinfection (3) and in Apo+ group (5).

models and viral strains may impact the process (Cymerys et al. 2012, Scrochi et al. 2013, Walter and Nowotny 1999).

We investigated whether the abortigenic AR8 EHV-1 strain may induce or prevent early and late apoptotic events in two different cell lines. We found that in both infected cell lines, apoptosis was increased by 18 h postinfection. This time period corresponds to the stage of the viral replication cycle when cell lysis takes place and viral progeny are released to the medium. We suggest that apoptosis and necrosis may occur at this moment, which would explain why DNA ladder fragmentation, the hallmark of apoptosis, was not clearly defined in our model.

We also observed that EHV-1 impacts negatively on the apoptotic process in MDBK and ED cells by 9 h postinfection (early infection time). ED cells were more susceptible to infection and modification of apoptosis than MDBK cells. Differences in cell line susceptibility to infection were reported by Turowska et al. (2010) who compared the effect of two EHV-1 abortigenic strains with different virulence on the cytoskeleton of ED and Vero cell lines; this supports the use of species-specific cell lines to improve infection and subsequent studies.

The antiapoptotic effect that we observed has been reported earlier for other alpha herpesviruses, such as BoHV-1 in MDBK cells (De Martino et al. 2003) and HSV-1 in human cell lines (Aubert et al. 2007), at early stages of replication cycle. On the other hand, Walter and Nowotny (1999) reported that necrosis was the mechanism of cell death caused by two different EHV-1 strains in Vero cells. Cymerys et al. (2012) showed that the virulence of EHV-1 strains in primary murine neurons determines extension of the antiapoptotic process and it may also characterize infection, i.e., whether productive or latent. Although these investigators reported both apoptotic and necrotic changes, they suggested that apoptosis prevails in EHV-1-infected murine neurons and therefore that apoptosis control may be the key mechanism for regulating the balance between productive and latent infection.

Interference with cellular apoptosis is associated with the expression of different viral proteins, as reported for different alpha herpesviruses. Therefore, it has been reported that gpG (Jin et al. 2003) and UL14 protein of BoHV-1 protect MDBK and human myeloma (K562) cell lines from sorbitol-induced apoptosis (De Martino et al. 2007). Similarly, HSV-1 exerts an antiapoptotic effect by expressing gpD (Sciortino et al. 2008), gpJ (Jerome et al. 2001), US3 protein kinases (Benetti and Roizman 2004), Us11 (Javouhey et al. 2008), g134.5 protein, ICP4 and ICP27 (Aubert and Blaho 1999). In addition, it has been shown that protein Us11 interferes with apoptosis in HeLa cells infected with HSV-1 (Javouhey et al. 2008); however, neither anti- nor proapoptotic viral proteins have been reported for EHV-1. Cymerys et al. (2012) reported that the protein expression of different caspases did not differ between infected mouse neuron primary cultures and control cell lines. Moreover, they demonstrated that viruses could survive in cell

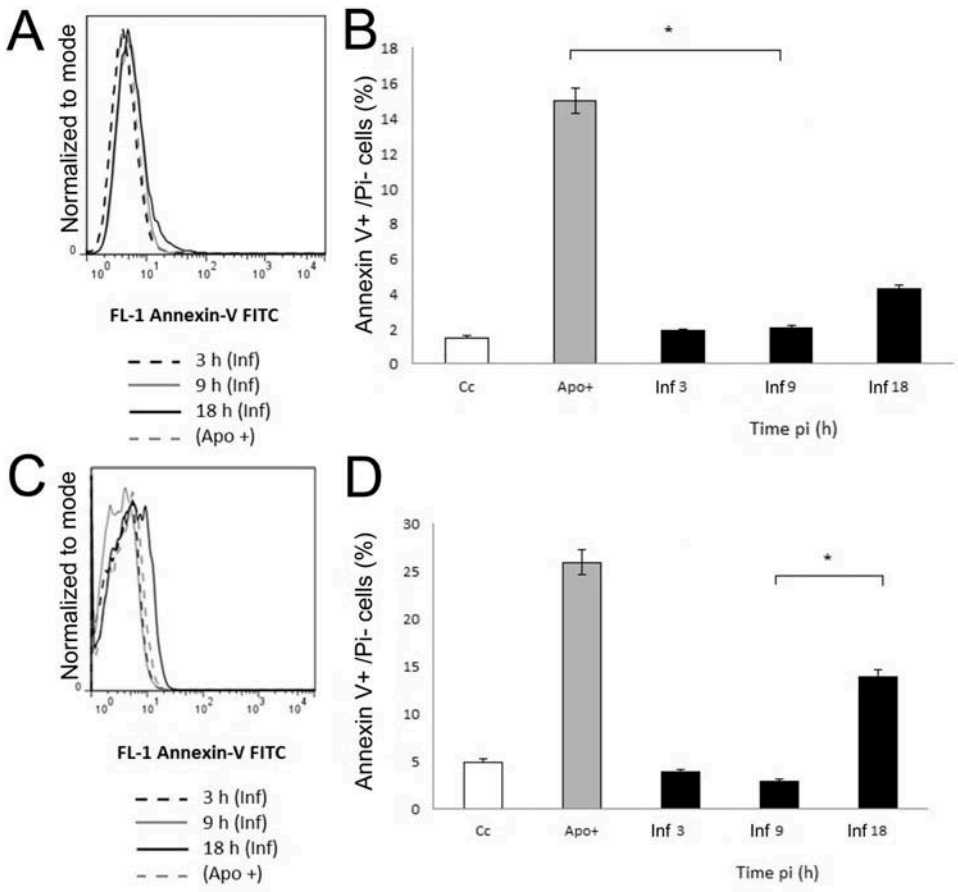

Fig. 6. Analysis of apoptosis by flow cytometry using annexin V/propidium iodide staining. a) Percentage of annexin V +/PI– at different postinfection times in MDBK cells. b) Statistically significant differences in MDBK cells in Inf group (*) at 9 h postinfection compared to Apo+. c) Percentage of annexin V+/PI– at different times postinfection in ED cells. d) Statistically significant differences in ED cells in Inf group (*) at 9 h compared to 18 h postinfection.

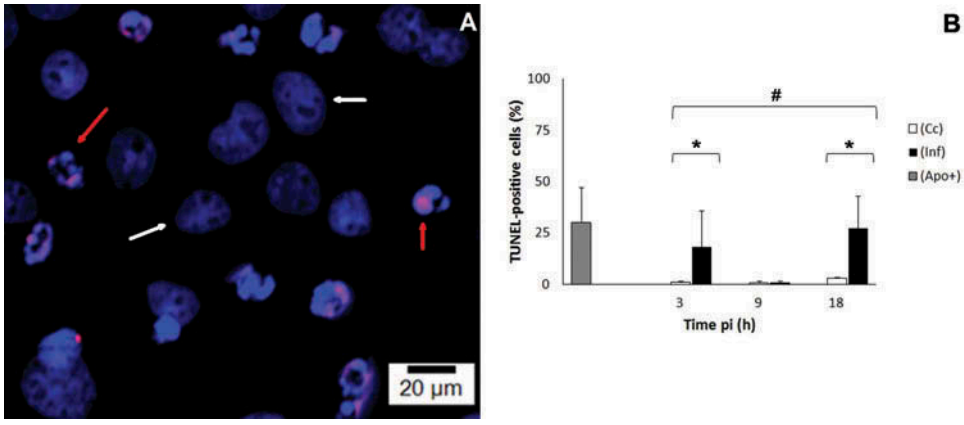

Fig. 7. Apoptosis in ED cells infected with an EHV-1 strain. Using TUNEL assay, DAPI counterstaining and confocal microscopy apoptosis was detected using an excitation 520–560 nm wavelength laser (green). Apoptosis was visualized in red. DAPI (excitation/emission wavelength was 358/461, blue) was used to identify cell nuclei. a) TUNEL-positive cells at 9 h Inf. White arrows point to normal cells, while red arrows point to apoptotic cells. b) Percentage of TUNEL-positive cells at different postinfection times. Statistically significant differences (*) between Inf and Cc groups, $p < 0.001$. Significant differences at 9 h postinfection (#) in Inf compared with 3 and 18 h postinfection, $p < 0.001$.

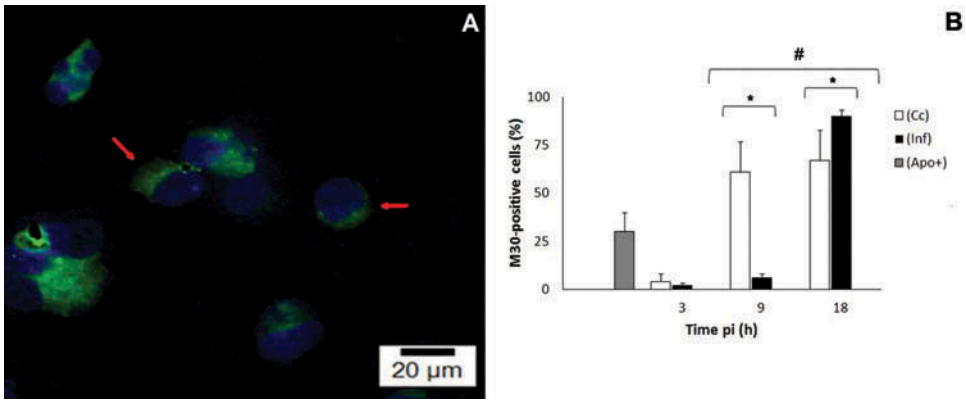

Fig. 8. Apoptosis in ED cells infected with an EHV-1 strain by immunofluorescence for cleaved cytokeratin 18. a) M30-positive cells of Inf group at 18 h postinfection. b) Percentage of M30-positive cells at different times postinfection. Statistically significant differences (*) between Cc and Inf groups, $p < 0.01$. Statistically significant differences (#) in Inf group at 9 h compared to 18 h postinfection.

cultures for eight weeks. Our findings, including our previous studies with EHV-1 HH1 strain in MDBK cells (Scrochi et al. 2013), support negative modification of apoptosis caused by alpha herpesvirus (Cymerys et al. 2012, De Martino et al. 2003, Deruelle et al. 2010).

Our findings contribute to understanding the potential of EHV-1 to increase efficiency during the replication phase at primary replication sites in natural hosts to increase the number of viral particles and to initiate viremia that leads to a systemic infection; however, further studies are required to elucidate the mechanisms and viral gene(s) and proteins involved in this type of interference. Studies concerning viral replication may bring new targets for antiviral therapy based on specific virus–host interaction.

Acknowledgments

This study was supported by grants from Argentinean Agency for the Promotion of Science and Technology (PICT 2011-1123), CIC-PBA (1376/12 and 1395/13), the Department for Science and Technology of the National University of La Plata (11-V188 and 11-V221) and CONICET (PIP 11220120100189CO). We would like to thank the technicians Mr. Claudio A. Leguizamón and Mrs Adriana Conde for their supporting help, and Dr. Pablo Martino for the proofreading of the manuscript.

Declaration of interest: The authors report no conflicts of interest. The authors alone are responsible for the content and writing of this paper.

References

Allen GP, **Kidd JH**, **Slater JD**, **Smith KC** (2004) Equid herpesvirus-1 (EHV-1) and -4 (EHV-4) infections. In: Coetzer JAW, Tustin RC, Eds. *Infectious Diseases of Livestock*. Oxford Press, Cape Town, South Africa. pp. 829–859.

Aubert M, **Blaho JA** (1999) The herpes simplex virus type 1 regulatory protein ICP27 is required for the prevention of apoptosis in infected human cells. ***J. Virol***. 73: 2803–2813.

Aubert M, **Pomeranz LE**, **Blaho JA** (2007) Herpes simplex virus blocks apoptosis by precluding mitochondrial cytochrome c release independent of caspase activation in infected human epithelial cells. *Apoptosis* 12: 19–35.

Benetti L, **Roizman B** (2004) Herpes simplex virus protein kinase US3 activates and functionally overlaps protein kinase A to block apoptosis. *Proc. Natl. Acad. Sci. USA* 101: 9411–9416.

Cheung AK, **Chen Z**, **Sun Z**, **McCullough D** (2000) Pseudorabies virus induces apoptosis in tissue culture cells. *Arch. Virol*. 145: 2193–2200.

Cymerys J, **Slonska A**, **Godlewski MM**, **Golke A**, **Tucholska AA**, **Chmielewska A**, **Banbura MW** (2012) Apoptotic and necrotic changes in cultured murine neurons infected with equid herpesvirus 1. *Acta Virol*. 56: 39–48.

De Martino L, **Marfe G**, **Di Stefano C**, **Pagnini U**, **Florio S**, **Crispino L**, **Iovane G**, **Macaluso M**, **Giordano A** (2003) Interference of bovine herpesvirus 1 (BHV-1) in sorbitol-induced apoptosis. *J. Cell. Biochem*. 89: 373–380.

De Martino L, **Marfe G**, **Irno Consalvo M**, **Di Stefano C**, **Pagnini U**, **Sinibaldi-Salimei P** (2007) Antiapoptotic activity of bovine herpesvirus type-1 (BHV-1) UL14 protein. *Vet. Microbiol*. 123: 210–216.

Deruelle MJ, **De Corte N**, **Englebienne J**, **Nauwynck HJ**, **Favoreel HW** (2010) Pseudorabies virus US3-mediated inhibition of apoptosis does not affect infectious virus production. ***J. Gen. Virol***. 91: 1127–1132.

Fuentealba NA, **Sguazza GH**, **Eöry ML**, **Valera AR**, **Pecoraro MR**, **Galosi CM** (2011) Genomic study of Argentinean Equid herpesvirus 1 strains. *Rev. Arg. Microbiol*. 43: 273–277.

Galosi CM, **Vila Roza MV**, **Pecoraro MR**, **Echeverría MG**, **Corva S**, **Etcheverrigaray ME** (2001) A polymerase chain reaction for detection of equine herpesvirus-1 in routine diagnostic submissions of tissues from aborted fetuses. *J. Vet. Med. B. Infect. Dis. Vet. Public. Health* 48: 341–346.

Galvan V, **Brandimarti R**, **Roizman B** (1999) Herpes simplex virus 1 blocks caspase-3-independent and caspase-dependent. *J. Virol*. 73: 3219–3226.

Honess W, **Roizman B** (1974) Regulation of herpesvirus macromolecular synthesis. Cascade regulation of the synthesis of three groups of viral proteins. *J. Virol*. 14: 8–19.

Javouhey E, **Gibert B**, **Arrigo AP**, **Diaz JJ**, **Diaz-Latoud C** (2008) Protection against heat and staurosporine mediated apoptosis by the HSV-1 US11 protein. *Virology* 376: 31–41.

Jerome KR, **Chen Z**, **Lang R**, **Torres MR**, **Hofmeister J**, **Smith S**, **Fox R**, **Froelich CJ**, **Corey L** (2001) HSV and glycoprotein J inhibit caspase activation and apoptosis induced by granzyme B or Fas. *J. Immunol*. 167: 3928–3935.

Jin L, **Peng W**, **Perng GC**, **Brick DJ**, **Nesburn AB**, **Jones C**, **Wechsler SL** (2003) Identification of herpes simplex virus type 1 latency-associated transcript sequences that both inhibit apoptosis and enhance the spontaneous reactivation phenotype. *J. Virol*. 77: 6556–6561.

Longo M, **Fiorito F**, **Marfè G**, **Montagnaro S**, **Pisanelli G**, **De Martino LG**, **Iovane G**, **Pagnini U** (2009) Analysis of apoptosis induced by caprine herpesvirus 1 in vitro. *Virus Res*. 145: 227–235.

Miles DH, **Thakur A**, **Cole N**, **Willcox MDP** (2007) The induction and suppression of the apoptotic response of HSV-1 in human corneal epithelial cells. *Invest. Ophthal. Vis. Sci*. 48: 789–796.

Munger J, **Chee A**, **Roizman B** (2001) The US3 protein kinase blocks apoptosis induced by the *d*120 mutant of herpes simplex virus 1 at a pre mitochondrial stage. *J. Virol*. 75: 5491–5497.

Pagnini U, **Montagnaro S**, **Sanfelice di Monteforte E**, **Pacelli F**, **De Martino L**, **Roperto L**, **Florio S**, **Iovane G** (2005) Caprine herpesvirus-1 (CapHV-1) induces apoptosis in goat peripheral blood mononuclear cells. *Vet. Immunol. Immunopathol*. 103: 283–293.

Perng GC, **Jones C**, **Ciacci-Zanella J**, **Stone Henderson G**, **Yukht A**, **Slanina SM**, **Hofman FM**, **Ghiasi H**, **Nesburn AB** (2000) Virus-induced neuronal apoptosis blocked by the herpes simplex virus latency-associated transcript. *Science* 287: 1500–1503.

Reed LJ, **Muench H** (1938) A simple method of estimating fifty percent end points. *Am. J. Hyg*. 27: 493–497.

Sciortino MT, **Medici MA**, **Marino-Merlo F**, **Zaccaria D**, **Giuffre-Cuculletto M**, **Venuti A**, **Grelli S**, **Bramanti P**, **Mastino A** (2008) Involvement of gD/HVEM interaction in NF-kB-dependent inhibition of apoptosis by HSV-1 gD. *Biochem. Pharmacol*. 76: 1522–1532.

Scrochi MR, **Zanuzzi CN**, **Muglia CI**, **Fuentealba NA**, **Nishida F**, **Gimeno EJ**, **Barbeito CG**, **Portiansky EL**, **Galosi CM** (2013) Interferencia del herpesvirus equino1 (EHV-1) en la apoptosis inducida. *In. Vet*. 15: 83–91.

Słonska A, **Cymerys J**, **Godlewski MM**, **Dzieciatkowski T**, **Tucholska A**, **Chmielewska A**, **Golke A**, **Banbura MW** (2014) Equine herpesvirus type 1 (EHV-1)-induced rearrangements of actin filaments in productively infected primary murine neurons. *Arch. Virol*. 159:1341–1349.

Soboll Hussey G, **Ashton LV**, **Quintana AM**, **Lunn DP**, **Goehring LS**, **Annis K**, **Landolt G** (2014) Innate immune responses of airway epithelial cells to infection with equine herpesvirus-1. *Vet. Microbiol*. 170: 28–38.

Turowska A, **Godlewski MM**, **Dzieciatkowski T**, **Chmielewska A**, **Tucholska A**, **Banbura M** (2010) Opposite effects of two different strains of equine herpesvirus 1 infection on cytoskeleton composition in equine dermal ED and African green monkey kidney vero cell lines: application of scanning cytometry and confocal-microscopy-based image analysis in a quantitative study. *Arch. Virol*. 155: 733–743.

Walter I, **Nowotny N** (1999) Equine herpes virus type 1 (EHV-1) infection induces alterations in the cytoskeleton of vero cells but not apoptosis. *Arch. Virol*. 144: 1827–1836.